CHAPTER 3

Artificial cloud generation

Based on the observations carried out during the BBC campaign, various impacts on cloud radiative smoothing are discussed in section 5. The results are verified with 3d RT simulations. In order to start these simulations realistic cloud fields and microphysical parameters need to be generated. Various cloud generators are discussed in the literature. In the following sections, three generators are presented which cover a wide range of possible procedures and which are utilised in this work. The cloud generators applied in this study produce either cloud top and cloud base heights or liquid water content (LWC). Sections 3.4 and 3.5 present approaches how either the geometrical or the LWC data can be converted to microphysical parameters needed for 3d RT.

3.1. Fourier clouds

Probably the most commonly used cloud generator is based on Fourier transformations. The major advantages of these kind of generators are that they are easy to handle with, they produce statistically well defined output fields and they are very efficient with respect to computation time. The main disadvantages are the statistical nature of the output which characterises reality with a few and in most cases unsufficient parameters, and the non-physical basis of the computation.

In the first step of generating Fourier clouds, normally distributed (Gaussian) noise is produced and transformed into complex values to allow calculations in Fourier space. This complex noise is then multiplied with a filter of kind $k^{-\beta}$. k is the frequency and β a real number. The product is subjected to an inverse Fourier transformation into physical space. Any required standard deviation and mean can be defined and multiplied, respectively added to the interim result. The so generated field has exactly the predefined standard deviation and mean and show a spectral behaviour of slope β. This approach is introduced by *Barker and Davies* (1992) where a more detailed description can be found, and is widely used in 3d RT studies to produce optical and/or geometrical thickness fields (e.g. *Iwabuchi and Hayasaka*, 2002).

Here, the Fourier cloud generator is extended to allow the incorporation of cloud top and cloud base variability. In order to achieve this, two Fourier fields are computed, both driven with the exact same random numbers. One Fourier field is considered as the geometrical thickness field, after the mean geometrical thickness $\langle H \rangle$ was added and a certain standard deviation was multiplied. The other field can either be treated as the cloud top or cloud base height field. Here, the required standard deviation, either σ_{cbh} or σ_{cth}, is multiplied but the mean cloud top or base height is defined by an average height of the cloud and $\langle H \rangle /2$. Both Fourier fields are combined by shifting the geometrical thickness columns according to either the cloud top or base height. The standard deviation multiplied to the geometrical thickness field is the sum of σ_{cth} and σ_{cbh}. The corresponding filter is related to either cloud top or cloud base height through the corresponding $\beta_{cth,cbh}$. If $\beta_{cth} \neq \beta_{cbh}$, one of both slopes and standard deviations cannot be maintained. In this case the user must specify if either cloud top or base height is forced to meet the requirements.

The procedure is outlined in Figure 3.1, where exemplary the cloud top height variability is forced. In Figure 3.1a the starting fields, the geometrical thickness and cloud top height field, are shown. Figure 3.1b gives the final cloud field after the columns were shifted according to the cloud top height.

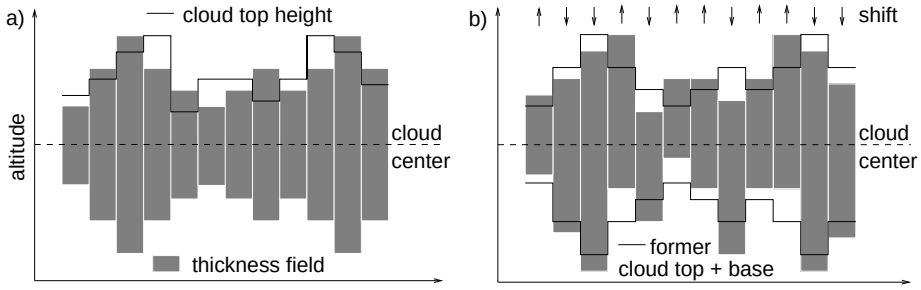

FIGURE 3.1. Sketch to explain the procedure of generating Fourier clouds. The starting fields, geometrical thickness and cloud top height, are given in Fig. a while Fig. b shows the cloud columns after the shift of columns according to requested cloud top variability.

Numerical difficulties may arise because the two Fourier fields contain random real numbers. In contrast, the user of the 3d RT model presented in section 4 must define vertical grid box sizes which are constant over the whole domain. This may result in deviations from requirements and may introduce noise at small scales.

These kind of Fourier clouds would make the systematic investigation of the effect of cloud top and base height variability on RT possible.

3.2. Surrogate clouds

A more sophisticated cloud generator is based on Iterative Amplitude Adapted Fourier Transform (IAAFT) surrogates, hereafter named surrogates. The iterative method relies on one or two measured data sets, e.g. liquid water path (LWP) and/or cloud top height. The values of their time series are dedicated as amplitudes in this section. The method requires the power spectrum and the amplitude distribution of the parameter of interest to generate a new realisation of the input. Surrogates are discussed in detail by *Schreiber and Schmitz* (2000) and *Venema et al.* (2004).

Starting point of IAAFT is a random shuffle of the original data set, yielding r_n^0. After taking the Fourier transformation of this processed set, the square of the Fourier coefficients are replaced by those of the original power spectrum. The inverse transformation is carried out by conserving the phases as derived from the transformation to Fourier space. The so determined data set d_n is sorted by magnitude in ascending order and replaced by the original, sorted data set a. The replacement is done by rank ordering: $r_n^1 = a_{\mathrm{rank}(d_n)}$ ($n = 1, ..., N$ and N: number of data points), e.g. $\mathrm{rank}\,(d_n)$=4 if d_n is the fourth smallest element of the data set. This procedure is repeated until a certain accuracy is reached. The standard deviation between subsequent iteratives is normalised to the standard deviation of the input. The algorithm stops if the ratio of the standard deviations deviates by a certain percentage from one. The final result can be taken either after the last Fourier or amplitude adaption. Here, the time series after the last amplitude adaption is chosen assuming that the amplitudes are more important than the structure. The new field is characterised by almost identical spectral behaviour and amplitude distribution as the original data set. *Schreiber and Schmitz* (2000) outlined a way to iterate two time series simultaneously by taking the cross correlation into account. Exemplary surrogate clouds and the corresponding input fields are discussed in sections 5.1, 5.2, and 5.4.

The IAAFT is not capable to produce clouds fields that reflect asymmetric structures, since the surrogate cloud is on average symmetric. Sharp rises and slow drops as well as Bernard cells cannot be be generated but are frequently found in nature. In addition, problems arise, if cumulus clouds are generated due to the discontinuity of the input.

The surrogate clouds are validated by *Venema et al.* (2004). They made surrogate clouds based on LES simulations and found excellent agreements if the radiative properties

of the surrogate and the LES cloud are compared. Differences have been identified for cumulus clouds.

All surrogate clouds presented in the following sections were provided by Victor Venema, MIUB. Here, the sorting of the original data sets, i.e. cloud top height and geometrical thickness, was binned to increments of 10 m. In this way it is ensured, that artificial noise introduced by IAAFT can be neglected.

3.3. Large eddy simulations

The large eddy simulation (LES) model used in this section was developed by *Lafore et al.* (1998). The simulations which form the starting point of the investigation of vertical and horizontal layering and averaging effects, were performed by Frederick Chosson, CNRM/Meteo France. The LES model is named Meso-NH Atmospheric Simulation System (Meso-NH). The model aims at the solution of the Navier-Stokes equation under atmospheric conditions on scales between mesoscale movements (e.g. movemement of a low pressure system) and the dissipation scale (a few centimeters). Everything below the smallest scale is either neglected or parameterised. The Meso-NH is an inelastic, non-hydrostatic LES model that allows vertical movement (e.g. driven by convection): The time dependence of the vertical moment is not neglected. All system variables are freed from their average, so that the Navier-Stokes equation is solved for the average (hydrostatic) and perturbed (non-hydrostatic) part. The initial state is defined by (sea-)surface temperature and pressure as well as profiles of total humidity (sum of liquid water, ice, and water vapour), windvector, and liquid water potential temperature θ_L. To reduce computational efforts perturbation is added to θ_L. At every time step (0.5 s) the soil scheme (*Noilhan and Planton*, 1989 and *Noilhan and Mahfouf*, 1996) is activated, and all three moments and the long-wave cooling and solar heating rates (using the radiation scheme of ECMWF) are determined at every grid point. The sun is considered to be time dependent, and a total runtime of three hours is typical. At the top boundary the Meso-NH is extended by a specific lid which absorbs vertical motions and relaxes prognostic variables to large-scale means. The lateral boundary condition is considered to be cyclic. The Meso-NH does not contain a microphysical model, i.e. no nucleation, droplet activation or droplet growth is considered, and therefore, the model is not capable of providing droplet spectra. Instead, LWC is calculated by transforming all relative humidity that reaches saturation to LWC. To avoid interactions between cloud structure and domain size, the model needs a maximum horizontal size of 10 km while the smallest scale is set to 50 m for both horizontal directions. The vertical resolution varies between 10 m and 50 m with the finest resolution in the cloud and inversion layer. The top of the domain reaches 1.5 km.

Figure 3.2 gives two examples of LWP fields simulated with the Meso-NH model. Figure 3.2a shows the result after 1:15 hours (stratus) and Figure 3.2b after 3 h (cumulus) of simulation while Figures 3.2c and d show corresponding LWC transects. The cloud fraction and the mean LWP values are 0.97 and 13 g m^{-2} (stratus) and 0.83 and 7 g m^{-2} (cumulus), respectively. The cloud fraction determination is based on the assumption that LWP values smaller than 0.1 g m^{-2} are considered cloud free. These two LES fields form the basis of the investigations carried out in section 6.

The initial state is oriented at the situation observed on 09 July 1997 (ACE2 campaign, *Brenguier et al.*, 1999). The LES simulations are validated against the findings of *Brenguier et al.* (2003). The statistics of LWC and geometrical thickness are in very good agreement (see *Chosson et al.*, 2004).

3.4. The adiabatic microphysical model

This section provides an outline for the generation of microphysical parameters, i.e. volume extinction coefficient, single scattering albedo, and phase function, for 3d RT simulations assuming adiabaticity. It is oriented at *Schüller et al.* (2003).

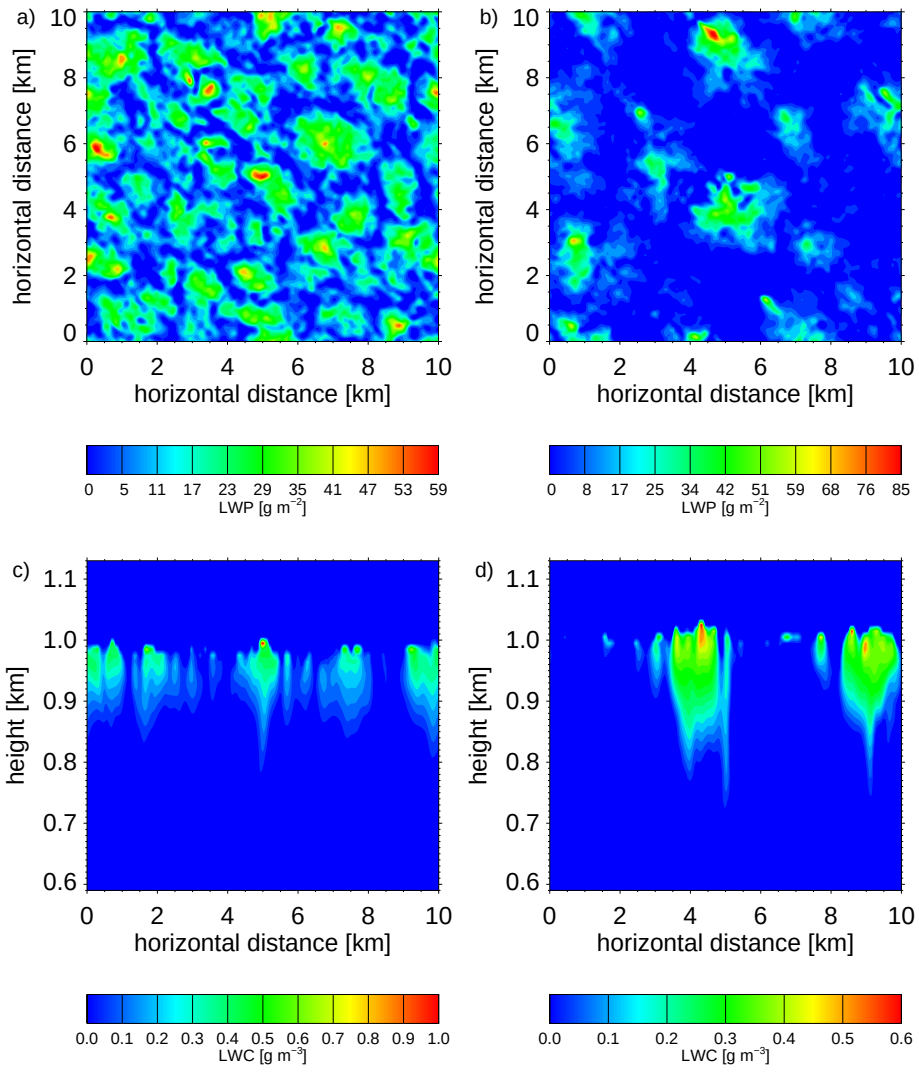

FIGURE 3.2. Two LWP fields, simulated with Meso-NH (Figs. a and c) and corresponding horizontal transects of LWC, taken at 5 km (Figs. b and d).

If we assume that the activation is completed at cloud base, approximately ten meters above cloud base, then the cloud droplet growth can be determined by (*Brenguier*, 1991):

$$\frac{\mathrm{d}r^2}{\mathrm{d}t} = 2BS \tag{3.1}$$

with r being the droplet radius, S the supersaturation and B a function of temperature and pressure. It follows from Eq. 3.1 that the surface growth rate remains constant in time, or here, in height above cloud base (in contrast to the growth of the radius). In consequence, if a plot of the droplet distribution versus squared radius is considered, the shape of the distribution does not change during the rise of the parcel. The spectrum is simply translated to higher r^2 values. The shift is parameterised with β^2. This parameter can be used to calculate the droplet surface distribution at any height above cloud base if the initial distribution is given. The initial profiles were determined by *Schüller et al.* (2003) for a discrete set of droplet number concentrations (eight values between 50 and

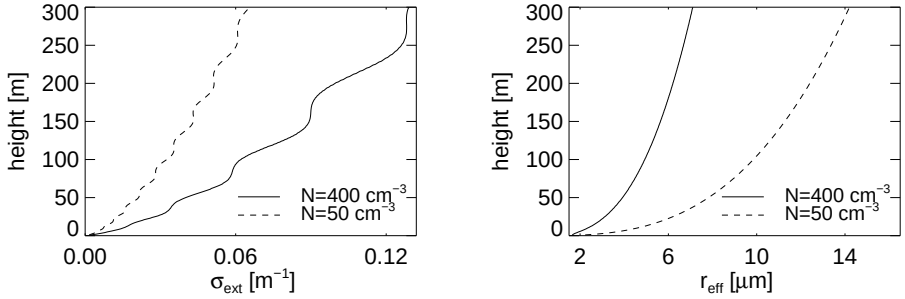

FIGURE 3.3. Volume extinction coefficient σ_{ext} (left panel) and effective radius r_{eff} (right panel) versus height above cloud base for two different droplet number concentrations.

400 cm^{-3}). N=50 cm^{-3} characterises a maritime, clean air mass and N=260 cm^{-3} a continental, polluted air mass. The spectra are fitted to measured droplet size distributions and are significantly narrower than usual distributions used for RT simulations (*Pawlowska and Brenguier*, 2000 and *Schüller et al.*, 2003).

If adiabaticity and the condensation rate c_w are given, the linear increase of liquid water content with height h, $\mathrm{LWC}\,(h) = c_w\,h$, can be used to determine $\beta^2\,(h)$. Utilising the initial profile for a given N and a table of corresponding $\beta^2\,(h)$, Mie theory is used to calculate σ_{ext}, ω_0, and $\tilde{\beta}$.

Exemplary profiles of the effective radius and the volume extinction coefficient for two different droplet number concentrations, N=50 and 400 m^{-3}, are given in Figure 3.3. While σ_{ext} increases continuously with height above cloud base, the increase of r_{eff} stagnates with increasing height. σ_{ext} is generally larger for larger N. r_{eff} is smaller in this case.

If artificial cloud geometries are available, e.g. through artificial cloud generation as discussed in sections 3.1 and 3.2, and if adiabaticity is assumed, the β^2-scheme can be used to calculate the microphysical parameters: The height above cloud base is used to derive the appropriate parameters.

3.5. Mixing scheme

It was mentioned in section 4 that the 3d RT model requires the single scattering albedo, the volume extinction coefficient, and the phase function at every grid box as input. In order to provide the model with these parameters the adiabatic assumption (section 3.4) may not hold if LWC fields simulated with Meso-NH are utilised. The LWC profiles can significantly differ from adiabatic predictions. A few examples are given in Figure 6.1. In this section the processes responsible for these discrepancies are discussed, and a simple mixing scheme is presented to model the required input parameters for the RT simulations on the basis of realistic LWC fields.

A realistic modelling of ω_0, σ_{ext}, and $\tilde{\beta}$ is a challenging task, since it requires the knowledge of the droplet spectrum at each grid point. In order to compute droplet spectra, the LES model should include the transport of aerosols, nucleation and droplet activation. Many bins of cloud condensation nuclei and droplets have to be introduced and need to be estimated at every grid box. Fine spatial resolutions and small time steps are required to resolve the underlying physical processes, especially if mixing between cloud and its environment occurs. *Brenguier and Grabowski* (1992) investigated the effect of mixing on the droplet spectrum by applying a 2d dynamical model with a simplified aerosol scheme. They computed the droplet spectra and found a wide variability of spectra: In addition to adiabatic results (narrow and monomodal spectra) multimodal and broad spectra were

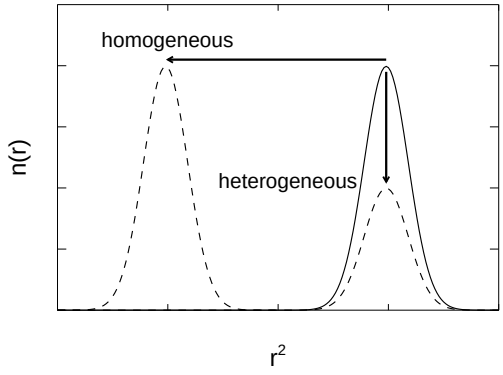

FIGURE 3.4. Cloud droplet number distribution versus squared radius (sketch). The effect of homogeneous and heterogeneous mixing on cloud droplet number distributions is demonstrated. The solid line gives the adiabatic distribution, the dashed lines the distribution after mixing and the arrows the change in radius (homogeneous) or cloud droplet number concentration (heterogeneous).

observed in old parcels and at cloud periphery. The deviation from adiabatic predictions is a frequent observation in their simulations.

Since the droplet spectra are not provided by Meso-NH, a mixing scheme is introduced which allows the interpretation of the LWC field in order to determine ω_0, σ_{ext}, and $\tilde{\beta}$. The mixing scheme differentiates between two scenarios, if LWC differs from adiabatic predictions, e.g. by turbulent mixing of dry air into cloudy parcels: the heterogeneous and homogeneous mixing (*Baker et al.*, 1980). It is assumed that the time constant for evaporation is smaller than for the mixing process with regard to the heterogeneous case . In the diluted parts cloud droplets of all sizes completely evaporate until the entrained air is saturated. Undiluted cloud parts are unaffected by this process. This leads to a reduction of the cloud droplet number concentration and leaves the effective radius constant. In the homogeneous case, the time constant for turbulent mixing is larger than for evaporation. Potential inhomogeneities, created by the mixing process, are smoothed out before evaporation starts. All cloud droplets experience the same water vapour deficit. The consequence is that all cloud droplets within the entrained field are reduced in size, according to Eq. 3.1, without a change in cloud droplet number concentration. The effect of both mixing schemes on cloud droplet number concentration is illustrated in Figure 3.4.

In the previous section a procedure was outlined which allows the calculation of ω_0, σ_{ext}, and $\tilde{\beta}$ by assuming adiabaticity. A particular consequence is the linear increase of LWC with height above cloud base. This procedure and the linear behaviour of LWC form still the basis for the determination of the input parameters for RT calculations if mixing is considered. Here, the interpretation of the results is changed in the following way: In case of homogeneous mixing, the liquid water content of the LES model, LWC$'$, is transformed to an adiabatic height above cloud base: $h = \mathrm{LWC}'/c_w$. h defines the values for $\omega_0(h)$, $\sigma_{ext}(h)$, and $\tilde{\beta}(h)$. With regard to heterogeneous mixing, the cloud droplet number spectrum $n'(r^2)$ which corresponds to the considered LWC$'$, is related to the adiabatic cloud droplet number spectrum by a constant factor: $n'(r^2) = fn(r^2)$ (see Fig. 3.4). The integral of the cloud droplet number spectrum is related to LWC and σ_{ext}. This allows the determination of f: $f = \mathrm{LWC}'/\mathrm{LWC}$ with LWC being the adiabatic liquid water content. If f is known, σ'_{ext} can be calculated by $\sigma'_{ext} = f\sigma_{ext}$. With the help of the height above cloud base, $h = \mathrm{LWC}/c_w$, ω_0, σ_{ext}, and $\tilde{\beta}$ are received. Heterogeneous mixing holds a problematic aspect: In case of homogeneous mixing LWC is a function of

effective radius with locally fixed N and c_w. If heterogeneous mixing is considered LWC is a function of N with locally fixed r_{eff} and c_w. Under the adiabatic assumption N and c_w are constant. Instead, r_{eff} is a function of height above cloud base. Here, not the actual cloud base of the LES field is meant but the cloud base at the time of cloud formation with possible alterations due to cloud movements. This is an unknown quantity in most cases. In general two approximations are applicable: 1) The local cloud base is used assuming that cloud base has not changed in time significantly, and 2) the 1% percentile cloud base is conducted.

Another approach is possible, if the evolution of the LWP field with time is documented (see Figure 3.2). It is possible to calculate a theoretical cloud base on the basis of local thermodynamic parameters (*Stull*, 2003). A comparison of the theoretical and observed cloud base (cloud field 1:15 h after initialisation) revealed a large coincidence which supports the application of option 1) in this case. The local cloud base is utilised for LWC(3 h), if the actual cloud base is lower than the cloud base of LWC(1:15 h). If this is not given, the local cloud base of LWC(1:15 h) is used.

Numerical problems arise in case of homogeneous mixing because the interpretation of non-adiabaticity is done in terms of height above cloud base. This height depends on LWC$'$ and may not correspond to an equal height value found in the adiabatic calculations. To avoid this LWC$'$ is interpolated to a resolution of 1 m, and the adiabatic parameters are calculated for a layer thickness of 1 m. After application of the mixing scheme, σ_{ext} is averaged over the required layer thickness while $\tilde{\beta}$ and ω_0 are directly determined for the required resolution.

In case of heterogeneous mixing and for LWC$'$>LWC the approach is very unlikely to happen in nature: Non-activated cloud droplet nuclei need to be activated and grow by condensation until they reach the assumedly constant effective radius. However, in the following all deviations from adiabaticity are interpreted as produced either by pure homogeneous or pure heterogeneous mixing.

One effect of the mixing scheme is that the optical thicknesses for both mixing cases are in general not identical. Using the definition of f, the ratio of the optical thicknesses related to homogeneous and heterogeneous mixing is proportional to $\frac{\tau_{hom}}{\tau_{het}} \sim 1/f^{4/3}$. Additionally, the optical thickness of the homogeneous mixing depends on a change in height, fH. In consequence, τ_{hom} is larger than τ_{het} if $f < 1$ (subadiabatic profiles) and vice versa (*Chosson et al.*, 2004).

A simple theoretical plot may give reason to prefer heterogeneous mixing as the most probable mixing process taking place in nature: The entrained undersaturated air enters the cloud as blobs or turbulent filaments. They produce sharp water vapour gradients between them and the cloudy areas which result in evaporation of the droplets in the vicinity of the entrained air. In fact, *Baker et al.* (1980) found a good agreement between laboratory measurements and numerical predictions of cloud droplet spectra assuming heterogeneous mixing. A recent study provides experimental evidence that in stratocumulus clouds heterogeneous mixing is the dominant mixing feature (*Brenguier et al.*, 2000).